The Rice Haptic Rocker: Altering the Perception of Skin Stretch through Mapping and Geometric Design

Janelle P. Clark, Sung Y. Kim, and Marcia K. O'Malley

Abstract— **Skin stretch haptic devices are well-suited for transmitting information through touch, a promising avenue in prosthetic research, addressing the lack of feedback in myoelectric designs. Rocker-based skin stretch devices have been proposed for sensory substitution and navigational feedback, but the designs vary in their geometry. Other works create torsional stretch, and utilize nonlinear mappings to enhance perception. This work investigates parameters of rocker geometry and mapping functions, and how they impact user perception. We hypothesize that perceptual changes are dependent on the choice of stretch increment sizes over the range of motion. The rocker geometry is varied with an offset between the rotational and geometric axes, and three rocker designs are evaluated during a targeting task implemented with a nonlinear or linear mapping. The rockers with no offset and a positive offset (wide) perform better than the negative offset (narrow) case, though the mapping method does not affect target accuracy.**

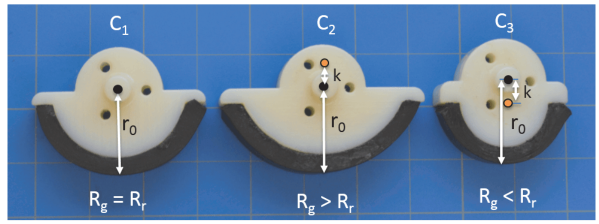

Fig. 1: Three rocker geometries previously proposed for skin stretch devices are compared to show how differences affect the ease with which the user discriminates positional change. The offset between the axis of rotation (black) and center of curvature (orange) results in wide (C_2), narrow (C_3), and neutral (C_1) geometries, all with the same radius of rotation in the neutral position, r_0.

I. Introduction

Myoelectric prostheses, controlled by measuring neural stimulation in the muscles, are becoming more prominent due to their lifelike appearance, finer manipulability, and smaller exertions to complete a motion compared to body powered designs [1]. The alternative, body powered designs, actuate by a harness with gross arm movements causing frictional interactions with the user's skin creating a form of sensory feedback. Despite discomfort, feedback through the harness of the hook aperture is viewed ultimately as an asset [2]. Due to the electronic control interfaces in myoelectric prostheses, the mechanical interactions with the amputee are eliminated. While this significantly increases the comfort [3], it also eliminates the corresponding feedback. The lack of sensory feedback has been identified as the key difference between myoelectric and body powered designs as early as 1975 [4]; however, commercial solutions are still not available. There are several neural interfaces in the research and clinical stages, ranging from relocating nerves through targeted muscle reinnervation [5], implanting electrodes in peripheral nerves with direct neural stimulation [6], or with implant interfaces directly with the brain [7]. These solutions create stimulations perceived on the phantom limb, however the expense of invasive devices, and a user preference for noninvasive solutions point to mechanical haptic devices as an effective short to medium term solution, replacing tactile sensory information from the amputated hand with tactile information in other areas of the body [8]. The ability to discern the aperture of the terminal device is a key benefit of body powered devices that the Rice Haptic Rocker is designed to provide in myoelectric prostheses.

Several modes of mechanical stimulation of the skin have been explored. Vibrotactile cues are popular feedback modes due to their compactness and low power consumption, portraying information through modulations of frequency or amplitude [9]. When compared to pressure feedback, vibrotactile had less resolution [10], motivating research in more mechanical interactions with the skin. Modality matching is an idea suggesting the most intuitive haptic mode to convey a given measurement is one that mimics the stimuli being measured [11], [12]. Implementations include applying normal loads to the arm [10], [13] and creating a torque about the elbow with an exoskeleton [14]. Skin stretch is another haptic mode, and the focus of this work, gently pulling the skin in order to provide a continuous cue informing the user of position and movement. The choice is motivated by the relationship between skin stretch and proprioceptive information in the human body through repeatable skin stretch patterns around actuated joints [15]. In functional tasks, the provision of skin stretch feedback has been shown to shorten training times, speed up classifications in grasping tasks [16], and reduce angular positional errors [17]. The Rice Haptic Rocker itself (pictured in Fig. 1) has already shown to be effective in object size discrimination tasks [18].

In addition to sensory substitution applications, skin stretch devices successfully convey motion guidance [19]–[21]. The success of skin stretch in conveying directional and position error cues also motivates the choice of this method for proprioceptive feedback in prosthetic systems, conveying

Janelle P. Clark, Sung Y. Kim and Marcia K. O'Malley are with the Department of Mechanical Engineering, Rice University, Houston, Texas, 77251 janelle.clark@rice.edu

absolute position information rather than positional error. The purpose of this work is to investigate design characteristics to enhance the performance of the Rice Haptic Rocker to be used in prosthetic feedback applications.

Rocker-based skin stretch devices have been proposed for sensory substitution and navigational feedback, but the designs vary in their geometry. A lateral skin stretch rocker was produced and tested in a pilot study within the MAHI Lab at Rice University, to create proprioceptive feedback for a gripper [22]. It has a frictional interface against the skin of the participants upper arm, linearly mapped to the grippers aperture. The geometry of the rocker has an axis of rotation set below the center of curvature, giving the geometry a wide appearance as illustrated in Fig. 2a. An alternate design was proposed by Chinello et al., and used a rubber interface for four small rockers, mounted in a bracelet, to stretch the skin laterally on the forearm [20]. This rocker design has an offset between the axis of rotation and the center of the geometric curvature as illustrated in Fig. 2b. The rotational axis is located above the center of curvature, giving the geometry a narrow appearance. The impact of geometric variations are assessed in this work,as shown in Fig. 1 in addition to changes in the mapping to the source.

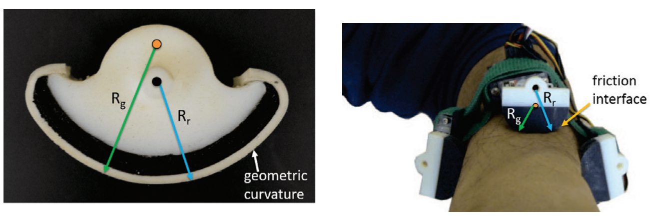

(a) Wide Rocker from MAHI Lab.

(b) Narrow Rocker, image adapted from [20].

Fig. 2: Previous skin stretch designs demonstrate two possible relationships of the rocker's center of curvature and the rotational axis.

The mapping between the sensed information and the motion of the rocker can also be varied. Work by Bark et al. used a nonlinear fifth order polynomial mapping to improve perception of rotational changes near the neutral position [17]. Their torsional skin stretch device conveyed positional information in a virtual task, where incremental changes were translated to the device through an s-curve function characterized by a steeper slope near the neutral position, corresponding to larger changes in rotation, and smaller increments at the extremes. The s-curve mapping counteracts the nonlinear behavior of the skin, which is projected to either enhance or mitigate the effects of geometric differences observed in the previous two works [20], [22].

II. Hardware Design

The purpose of a haptic feedback device is to convey specific, easily distinguished information to a user. The mechanical nature of skin stretch in the Rice Haptic Rocker and application in prosthetic systems leads to a particular importance of the mechanical design. In order to ensure positional changes of the rocker are easily perceived over the full range of motion, it should have good contact with the skin, the appropriate geometric curvature, and map to the prosthetic aperture in an intuitive way.

The fundamental principle by which the design of rocker geometries and mappings are considered is related to incremental arc lengths. The Rice Haptic Rocker is a skin stretch device, with a rotational axis parallel to the skin's surface, causing a lateral stretch of the skin. With each increment of rotation, the frictional interface pulls the skin by an amount equal to the arc length associated with the rocker's rotation. This incremental arc length can be modified two ways, by changing the geometry of the rocker, making it wider or more narrow, or by adjusting the mapping, redistributing the rocker's contact surface to move according to a nonlinear function of the source measurement input.

A. Instantaneous Arc Length Derivation

If the arc length, L, for a constant angular increment varies over the rocker's range of motion, the way it feels to the user will change. To investigate this relationship, three rocker designs are presented to illustrate two specifications that influence this instantaneous arc length. The first defines all three of the rockers as circular arcs with an equal instantaneous radius of rotation in the neutral position, $r_0 = 20$ mm. The second is an offset between the rotational and geometric axes in the second and third cases. As defined, the instantaneous radius at the neutral position, r_0, is the sum of the axis offset, k, and geometric radius of curvature, R_g. This criteria results in an adjustment in the geometric radius in the wider and narrow rocker case, as shown in Fig. 1, making the instantaneous radius of rotation a function of the angular position.

The instantaneous radius of rotation can be defined mathematically, leading to an understanding of the impact on the incremental arc length over the rocker's range of motion. The parameters in the rocker design are illustrated in Fig. 3, where the circular function represents the curvature of the rockers surface and the origin represents the axis of rotation.

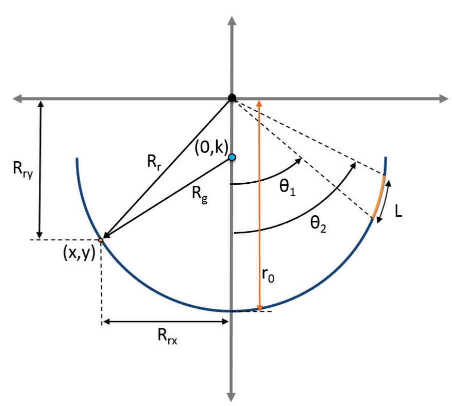

Fig. 3: The position of the geometric center of the rocker arc (blue) relative to the axis of rotation (black) impacts the instantaneous radius over the range of motion.

The geometric radius of curvature is defined by R_g, whose center is offset from the axis of rotation by the offset k, resulting in a distinct instantaneous radius of rotation, R_r. The rocker is assumed to be placed on the user's arm in the neutral position, with no stretch, where the axis of rotation and geometric center are in line perpendicular to the skin's surface. The negative y axis is then representative of θ equal to zero, and each point on the curve is associated with some angular position.

A point on the arc can be represented either as a function of the rotational radius and the angular position or by a function of the circular profile. The system of equations results in a closed form solution for the instantaneous rotational radius in (1), which can be used to calculate the incremental arc length between any two angular positions, (2). This is used to evaluate three rocker geometries shown in Fig. 1, where in C_1 the geometric center is coincident with the axis of rotation, and C_2 and C_3 have a geometric center above and below the axis of rotation, respectively.

$$R_r = kcos(\theta) + \sqrt{R_g^2 - k^2 sin^2(\theta)} \tag{1}$$

$$L = \int_{\theta_1}^{\theta_2} \sqrt{R_r^2 + \frac{dR_r}{d\theta}^2}\, d\theta \tag{2}$$

B. Rocker Implementation

The geometric differences in rockers from previous studies are represented through changes in the offset between the rotational and geometric axes. Since there is no offset in C_1, R_r is equal to R_g, a constant 20 mm over the entire range of motion. The offset magnitude is constant for both C_2 and C_3, where $|k| = 5$ mm, resulting in geometric radii of 25 mm and 15 mm respectively. The center offsets and radii for the three rocker designs are summarized in Table I.

TABLE I: Rocker Geometric Parameters

	C_1	C_2	C_3
r_0 [mm]	20	20	20
k [mm]	0	5	-5
R_g [mm]	20	25	15

The impact of the geometric differences between the rockers on the incremental arc length is shown in Fig. 5, where the rocker's range of motion is divided into one degree increments and the arc length within each increment is plotted. As expected, the delta arc length is constant for C_1 since the instantaneous rotation is constant. In C_2, the increment decreases at extreme values, and increases in the C_3 rocker case.

C. Mapping Design

The nonlinear mapping similar to the one proposed in the torsional skin stretch device [17] is now applied to lateral stretch rockers. A nonlinear mapping is an alternative way of modifying the arc length distribution throughout the rockers' range of motion. In Section II-B, it was assumed that the angular increment of the rocker was proportional to the hand aperture, and perceptual changes were attained by modifications in the rocker profile. The proportional relationship is referred to as a linear mapping, and is compared to the impact of a nonlinear mapping described by a logistic s-curve function, shown in (3). The nonlinear function maps a constant incremental change in the hand aperture to larger changes close to the rocker's neutral position and smaller ones at the extrema, similar to the geometric impact of C_2. This approach is based on the observation that skin is increasingly sensitive to small changes in stretch where a pre-stretch is present. The behavior is exaggerated in Fig. 4a to illustrate the behavior, but the actual function in Fig. 4b seems quite subtle. It is defined by only two coefficients, q and m. The rationale for this choice is outlined in Section II-D, where the arc length increments over the range of motion change drastically, allowing hypotheses to be made and help decipher the perceptual variables.

$$f(x) = \frac{m}{1 + e^{-qx}} \tag{3}$$

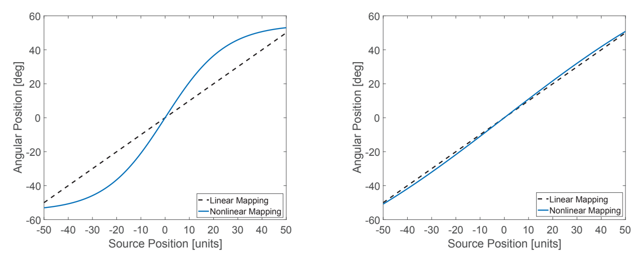

(a) Exagerated Mapping for Illustration.

(b) Actual Nonlinear Mapping

Fig. 4: The nonlinear mapping redistributes the rocker's position corresponding to a measurement of interest. The logistic function results in larger changes near the center and smaller changes at the extreme.

D. Geometry-Mapping Interaction

Although the impact of the nonlinear mapping seems minimal in Fig. 4b, Fig. 5 shows the substantial changes in the distribution of arc length between the two mappings. The curve amplifies the geometric impact of C_2, but also redistributes the rockers' surface area in C_1 and C_3 to reflect the same concave shape. Another visualization in Fig. 6 provides a physical representation of the difference in mapping for each of the geometries. If the changes in arc length are a valid method for design and predicting performance outcomes, the linear mapping C_2 should perform the best and C_3 have the lowest performance. The nonlinear mapping should improve performance for C_3, and perhaps C_2 as well.

Table II shows the mean arc length per one degree increments the linear mapping, $\bar{L}_{Lin}$, and an equal number of divisions for the nonlinear mapping, $\bar{L}_{NL}$. The results show that the geometry dominates the mean arc length increment overall, which is expected considering the increments must add up to a larger number for C_3 for the same number of increments in C_2 and C_1.

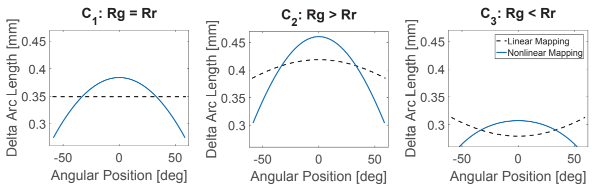

Fig. 5: The rocker geometry impacts the arc length stretching the skin with uniform rotational increments. Overall C_3 has the smallest increments, C_2 has the largest, and C_1 is intermediate.

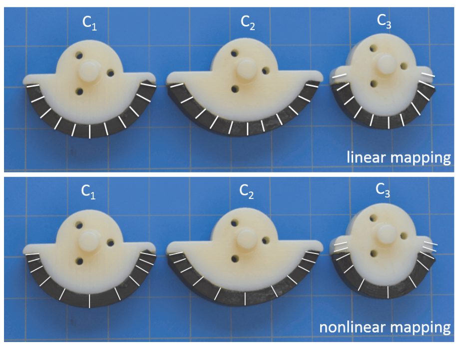

Fig. 6: The nonlinear mapping redistributes the arc length of the rocker for a constant input increment, with larger movements closer to the center and smaller ones farther away.

III. Methods

In order to compare and examine the effectiveness of modulating geometric and mapping parameters of the rocker in relation to tactile perception, we asked human users to perform a virtual target task. The position information was relayed through skin stretch with all three rockers and both mappings. We hypothesized that a concave relationship between the rocker position and the delta arc length would result in increased user perception. For geometric changes, the larger arc length increments toward the center in C_2 would result in the highest target accuracy, C_3 would be the lowest, and C_1 would be intermediate. For mapping modifications, the nonlinear mapping would result in lower positional errors compared to the linear mapping.

A. Experimental Participants

Twelve able-bodied subjects (age 23 ± 3 years, 4 female, 1 left handed) participated in the experiment. The participants did not claim any physical or cognitive impairment that could interfere with their ability to follow the instructions of the study, nor any pathology that could affect tactile sensation or muscular activity of the forearm. The methods and procedures described in this paper were carried out in accordance with the recommendations of the Institutional Review Board of Rice University with written informed consent obtained from all users.

TABLE II: Average Arc Length Increment for Each Rocker

	C_1	C_2	C_3
$\bar{L}_{Lin}$ [mm]	0.35	0.41	0.29
$\bar{L}_{NL}$ [mm]	0.34	0.40	0.29

B. Experimental Platform

A frame was constructed to secure the rockers against the forearm. The frame consists of two, nine inch t-slotted frame lengths, secured to a mechanical breadboard with three brackets and screws (1/4”-20). Two adjustable sliders with hand brakes held the 3D printed rocker mount with four brackets, screws, and nuts (1/4” - 20). The rocker mount and rockers were printed in a Connex Objet 260 printer with a hard abs-like plastic. The rocker was actuated by a servo (Hitec HS-5070MH), held in place with 2 socket head screws and nuts (M1.6 x 0.35 mm). The rocker subassembly was mounted so the bottom of the Rocker in the neutral position is offset 10 mm, d, from the bottom of the frame to allow appropriate pressure against the skin without contact with the rest of the frame. The rocker subassembly was made up of the rocker, and a six axis force transducer (ATI Nano17). All three rocker geometries were tested in this framework, each with a 3/16 inch (5 mm) neoprene foam strip to avoid slipping and increase comfort.

The perceptual task took place at a workbench with participants seated in front of monitor and keyboard. Headphones with pink noise prevented auditory cues from the rocker's servo. Participants were asked to place their right arm on the breadboard and adjust the seat height to their preference. The forearm was positioned flat on the breadboard, and the rocker 10 cm from the lunate bone [20]. The rocker was pressed against the forearm with an initial normal force of 2.5 N read by the ATI Nano17 force sensor. The rocker assembly was hidden by a black curtain causing participants to rely solely on the skin stretch feedback from the rocker during the target task. The experimental set up is shown in Fig. 7.

The target task was created with MATLAB and Simulink, utilizing QUARC visualization software, with five equally spaced, vertically aligned targets positioned at 48, 24, 0, -24, and -48 units, as shown in Fig. 8. The travel distance of the cursor per key press was constant within the trial, however the increment was varied between trials to ensure

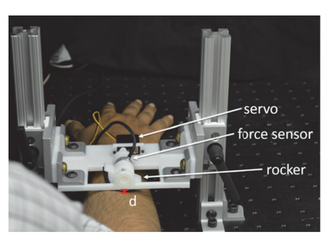

(a) Frame Set-Up

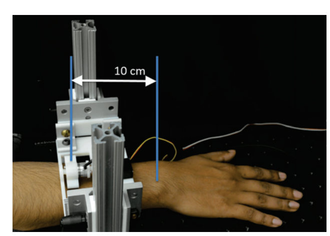

(b) Forearm Position.

Fig. 7: The participant is seated at the bench facing the monitor, their right arm is positioned under the skin stretch device so the rocker is 10 cm from the lunate bone.

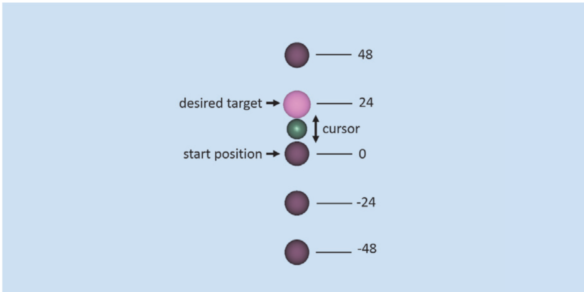

Fig. 8: The visualization for the perceptual task, the desired target blinks and the cursor is controlled using the keyboard.

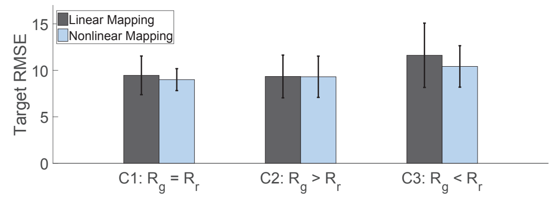

Fig. 9: The mean RMSE across all users for each of the 6 experimental conditions, error bars represent the RMSE standard deviation. The rocker geometry has a significant effect ($p = .014$), and C_3 has significantly higher errors compared to C_1 and C_2 ($p = .034$).

participants relied solely on the rocker sensation, rather than the number of key-presses, to reach the desired target. The increment varied randomly between 1, 2, 3, 4, or 6 units across trials. The coefficients for the nonlinear mapping had the values $q = 0.02$ and $m = 220$, producing the desired changes to the arc length distribution shown in Fig. 5. In the linear mapping each unit corresponded to one degree of rotation. The maximum allowable rocker rotation was $60°$, allowing participants to navigate up to $12°$ beyond the outer targets. Participants controlled the cursor using the 8 and 2 keys on the numeric pad with their left hand, pressing the enter key when they perceived the target was reached, ending the trial.

C. *Experimental Protocol*

The target task was completed for three rocker geometries and two mappings, for a total of six conditions. Three 1 hour sessions, each with one of the three rocker geometries, were assigned to participants in different orders, with two participants for each of the six permutations. There were two sets within each session, for the linear and nonlinear mapping. Half of participants completed the linearly mapped set first, and the other half completed the nonlinear mapped set first, to eliminate training bias or fatigue effects. Each set consisted of three phases: training, assessment, and a participant evaluation.

The training phase had two blocks. Training block I consisted of 60 trials during which the cursor was present on the screen at all times. Training block II had 60 trials as well, with no cursor present until after the subject completed the trial. After the participants indicated they reached the target, the cursor appeared briefly to make them aware of errors and allow for adjustments. The assessment phase consisted of twenty trials with no visual feedback. The cursor was not present during any trials, and responses were based solely on the skin stretch sensation. In the training and assessment phases, each target and each cursor increment combination were represented an equal number of times, randomly ordered in each phase.

IV. Results

Performance was quantified with the root mean squared error (RMSE) of the cursor position with respect to the desired target in the assessment phase. The mean RMSE was $9.2 \pm 1.8\%$ for C_1, $9.32 \pm 2.6\%$ for C_2, and $11.0 \pm 3.71\%$ for C_3. For the linear mapping the mean RMSE was $10.1 \pm 3.5\%$, and $9.6 \pm 2.2\%$ for the nonlinear mapping. Fig. 9 illustrates the performance in each condition.

Statistical analyses were performed to identify performance differences in rockers and mappings, as well as possible interactions between them. A 3×2 [Rocker (C_1; C_2; C_3) $\times$ Mapping (L; NL)] repeated-measures ANOVA was used to assess the RMSE across conditions. To adjust for sphericity deviations, a Huynh-Feldt (HF) adjustment was used. The analysis showed a difference in RMSE between the rocker geometries, $F(2,22) = 5.20$, $p = .014$, $\eta^2 = 0.32$. A contrast was used to test if the performance of C_3 was different than C_1 and C_2. The significant result, $t(11) = 2.43$, $p = .034$, suggests the performance for C_3 was lower than C_1 and C_2, with higher errors overall. Mapping, however, did not have a significant effect, and no significant interaction present between Rocker and Mapping.

V. Discussion

The goal of this experiment was to gain insight into factors which affect participant skin stretch perception, namely, the curvature of the rocker and the mapping used to correlate to prosthetic information. An s-curve nonlinear mapping between the hand aperture and the rocker position was used to improve performance by recognizing the expected tendency of detecting smaller changes in stretch with a pre-stretch already present. Both the linear and nonlinear mapping were applied to all three rockers, with no significant effects. This indicates the implemented mapping is not a viable method of impacting perception, though this does not bar alternative parameters or functions from creating effective results. The geometries, however, did result in performance changes.

The wider rocker, C_2, with the rotational axis set below the center of curvature, mimics the effect of nonlinear mapping, where a constant angular increment results in a decreased arc length of stretch. The narrow rocker, C_3, is the opposite, with increasing arc length segments at extreme angular positions. Under these considerations, C_3 should perform the worst, then C_1, and finally, C_2 should have superior performance.

The target task showed that C_3 does have the worst performance, which agrees with our initial hypothesis. The lack of a significant interaction with the type of mapping suggests that the problem may not simply be the changes in arc length, but in the mechanical interactions with the arm. As the rocker rotates, the instantaneous radius of curvature decreases, which causes a decreasing normal force. This decrease would also affect the shear forces present in the stretch, possibly influencing the user perception.

Another possible reason for C_3's poor performance, apart from the decreasing changes in arc length per increment, is the total arc length of the rocker over its full range of motion. The rockers were designed to all have an equal radius of curvature at the neutral position. Since the axis of rotation is above the center of curvature in C_3, the geometric radius of the rocker arc is smaller than the other cases, resulting in a smaller total arc length. This results in smaller increments in the linear and nonlinear cases compared to the other two. If this is the case it may cause issues for miniaturization, a desirable trait in prosthetic components, which are constantly streamlined to be lighter and less bulky.

VI. Conclusion

The objective of this work was to quantify the effect of two design parameters of rocker-based haptic skin stretch devices on human perceptual performance. One parameter, the nature of mapping information onto the rocker (linearly or nonlinearly) had no significant effect on performance in a targeting task. The second, the relative position of the rocker center of curvature and center of rotation did have a significant effect on performance. Results suggest that for positioning tasks, the center of curvature should be coincident or above the center of rotation for best perceptual performance. Further investigation into the parameters and function of the nonlinear mapping and the effect of the total stretch in each rocker are open for future work.

References

[1] A. Fougner, Ø. Stavdahl, P. J. Kyberd, Y. G. Losier, and P. A. Parker, "Control of upper limb prostheses: terminology and proportional myoelectric control a review," *IEEE Transactions on Neural Systems and Rehabilitation Engineering*, vol. 20, no. 5, pp. 663–677, 2012.

[2] S. L. Carey, D. J. Lura, and M. J. Highsmith, "Differences in myoelectric and body-powered upper-limb prostheses: Systematic literature review.," *Journal of Rehabilitation Research & Development*, vol. 52, no. 3, 2015.

[3] S. Millstein, H. Heger, and G. Hunter, "Prosthetic use in adult upper limb amputees: a comparison of the body powered and electrically powered prostheses," *Prosthetics and Orthotics International*, vol. 10, no. 1, pp. 27–34, 1986.

[4] T. Rohland, "Sensory feedback for powered limb prostheses," *Medical and Biological Engineering and Computing*, vol. 13, no. 2, pp. 300–301, 1975.

[5] T. A. Kuiken, P. D. Marasco, B. A. Lock, R. N. Harden, and J. P. Dewald, "Redirection of cutaneous sensation from the hand to the chest skin of human amputees with targeted reinnervation," *Proceedings of the National Academy of Sciences*, vol. 104, no. 50, pp. 20061–20066, 2007.

[7] J. Kubanek, K. Miller, J. Ojemann, J. Wolpaw, and G. Schalk, "Decoding flexion of individual fingers using electrocorticographic signals in humans," *Journal of Neural Engineering*, vol. 6, no. 6, p. 066001, 2009.

[6] G. S. Dhillon and K. W. Horch, "Direct neural sensory feedback and control of a prosthetic arm," *IEEE Transactions on Neural Systems and Rehabilitation Engineering*, vol. 13, no. 4, pp. 468–472, 2005.

[8] J. S. Schofield, K. R. Evans, J. P. Carey, and J. S. Hebert, "Applications of sensory feedback in motorized upper extremity prosthesis: a review," *Expert Review of Medical Devices*, vol. 11, no. 5, pp. 499–511, 2014.

[9] C. Cipriani, M. DAlonzo, and M. C. Carrozza, "A miniature vibrotactile sensory substitution device for multifingered hand prosthetics," *IEEE Transactions on Biomedical Engineering*, vol. 59, no. 2, pp. 400–408, 2012.

[10] C. Antfolk, M. D'Alonzo, M. Controzzi, G. Lundborg, B. Rosén, F. Sebelius, and C. Cipriani, "Artificial redirection of sensation from prosthetic fingers to the phantom hand map on transradial amputees: vibrotactile versus mechanotactile sensory feedback," *IEEE Transactions on Neural Systems and Rehabilitation Engineering*, vol. 21, no. 1, pp. 112–120, 2013.

[11] K. Kim, J. E. Colgate, J. J. Santos-Munné, A. Makhlin, and M. A. Peshkin, "On the design of miniature haptic devices for upper extremity prosthetics," *IEEE/ASME Transactions on Mechatronics*, vol. 15, no. 1, pp. 27–39, 2010.

[12] S. G. Meek, S. C. Jacobsen, and P. P. Goulding, "Extended physiologic taction: design and evaluation of a proportional force feedback system," *Journal of Rehabilitation Research & Development*, vol. 26, no. 3, pp. 53–62, 1989.

[13] P. D. Marasco, K. Kim, J. E. Colgate, M. A. Peshkin, and T. A. Kuiken, "Robotic touch shifts perception of embodiment to a prosthesis in targeted reinnervation amputees," *Brain*, vol. 134, no. 3, pp. 747–758, 2011.

[14] B. Gillespie, J. Baker, M. O'Malley, P. Shewokis, and J. L. Contreras-Vidal, "Functionally biarticular control for smart prosthetics," in *Proceedings of the IEEE Third Joint Eurohaptics Conference and Symposium on Haptic Interfaces for Virtual Environment and Teleoperator Systems*, pp. 627–628, 2009.

[15] D. F. Collins, K. M. Refshauge, G. Todd, and S. C. Gandevia, "Cutaneous receptors contribute to kinesthesia at the index finger, elbow, and knee," *Journal of Neurophysiology*, vol. 94, no. 3, pp. 1699–1706, 2005.

[16] A. Akhtar, M. Nguyen, L. Wan, B. Boyce, P. Slade, and T. Bretl, "Passive mechanical skin stretch for multiple degree-of-freedom proprioception in a hand prosthesis," in *Haptics: Neuroscience, Devices, Modeling, and Applications* (M. Auvray and C. Duriez, eds.), vol. 8619 of *Lecture Notes in Computer Science*, Springer, Berlin, Heidelberg, 2014.

[17] J. Wheeler, K. Bark, J. Savall, and M. Cutkosky, "Investigation of rotational skin stretch for proprioceptive feedback with application to myoelectric systems," *IEEE Transactions on Neural Systems and Rehabilitation Engineering*, vol. 18, no. 1, pp. 58–66, 2010.

[18] E. Battaglia, J. P. Clark, M. Bianchi, M. G. Catalano, A. Bicchi, and M. K. O'Malley, "The rice haptic rocker: skin stretch haptic feedback with the pisa/iit softhand," in *Proceedings of the IEEE World Haptics Conference*, 2017.

[19] A. L. Guinan, N. C. Hornbaker, M. N. Montandon, A. J. Doxon, and W. R. Provancher, "Back-to-back skin stretch feedback for communicating five degree-of-freedom direction cues," in *Proceedings of the IEEE World Haptics Conference*, pp. 13–18, 2013.

[20] F. Chinello, C. Pacchierotti, N. G. Tsagarakis, and D. Prattichizzo, "Design of a wearable skin stretch cutaneous device for the upper limb," in *Proceedings of the IEEE Haptics Symposium*, pp. 14–20, 2016.

[21] A. A. Stanley and K. J. Kuchenbecker, "Evaluation of tactile feedback methods for wrist rotation guidance," *IEEE Transactions on Haptics*, vol. 5, no. 3, pp. 240–251, 2012.

[22] A. Blank, C. A. Brookshier, and M. O'Malley, "Skin stretch feedback of gripper aperture for prosthetic hands in a grasp and lift task (work in progress)," in *Proceedings of the IEEE World Haptics Conference*, 2015.